Mesoscopic simulation for damage and failure of rock with double-fractures under dynamic compression

Mesoscopic simulation for damage and failure of rock with double-fractures under dynamic compression

Yue Yuan[1,2*], Jinlei Fu[3] and Jian Qin[3]

[1] Work Safety Key Lab on Prevention and Control of Gas and Roof Disasters for Southern Coal Mines, Xiangtan, Hunan, 411201, China

[2] Hunan Provincial Key Laboratory of Safe Mining Techniques of Coal Mines, Xiangtan, Hunan, 411201, China

[3] School of Resource, Environment and Safety Engineering, Hunan University of Science and Technology, Xiangtan, Hunan, 411201, China

[*]Corresponding author's e-mail: yuanyuekafu@163.com

Abstract. Aiming at instability of rock pillar subjected to dynamic load in underground mining, damage and failure process of rock with double-fractures under uniaxial dynamic compression was simulated by particle flow code (PFC). Mesoscopic damage variable was defined based on the number of fracture bonds between particles, and damage characteristics of the rock with double-fractures was analysed. Then change laws of rock peak strength, cracks distribution, accumulation and release of elastic strain energy were revealed, furthermore the internal cause for accelerated growth of rock sample microcracks post peak was obtained. The results show that the number of cracks on rock with double-fractures increases with the peak strength under uniaxial dynamic compression. Compared with large-size fractures, the rock sample with small-size fractures takes longer to reach peak strength and have higher bearing capacity. Additionally the number of microcracks on the rock sample is positively correlated with the mesoscopic damage variable (D), while the elastic strain energy accumulated at the peak and the peak strength are all negatively correlated with the length of fracture B.

1. Introduction

For underground mining, rock pillar is often in a uniaxial compression state and damaged. When the damaged rock pillar is affected by dynamic loads such as rock burst and blasting, sudden failure and mine disasters may occur. Therefore, the stability of rock pillar is related to stability and safety of the whole underground structure[1,2]. At present, the failure law of jointed rock mass can't be analysed quantitatively in theory[3-5], and the cost of laboratory test is high with long period, moreover it is difficult to effectively monitor microcracks of rock sample. While the discrete element particles flow code (PFC) can simulate the microcrack propagation on rock sample, which is more suitable for explaining the damage evolution process of rock in mechanism[6].

Many scholars have studied cracked rock by using PFC. Whether the crack closure has an effect on rock strength and failure characteristics was confirmed by Chen[7]. The relationship between peak strength of coplanar sandstone and coplanar fracture angle was discussed by Tian[8]. Li[9] pointed out that when two echelon fractures have an intersection angle, a certain shielding effect will occur in the crack propagation, resulting in increase of rock strength. Cao[10] investigated crack initiation and

coalescence under compression-shear loading, and observed three types of coalescence modes between intermittent fractures.

However, the above studies are not involved rock crack propagation and damage characteristics under different fracture size combinations. Therefore, in this paper the effect of fracture size on damage and failure of rock with double-fractures under uniaxial dynamic compression was simulated by PFC. Then the damage evolution characteristics, crack propagation and accumulation and release of elastic strain energy were analysed.

2. Numerical model and experimental scheme

2.1 Particle flow model of rock with double- fractures

The Linearpbond model is used in the PFC. The simulation of uniaxial compression is divided into three steps. Firstly a numerical test container is generated, secondly parameters for uniaxial compression with parallel bonds are set, and finally loading condition is executed. After repeated debugging, the mesoscopic parameters are obtained, as shown in table 1. A mechanical model of the underground rock pillar[1] is shown in figure 1(a). A rock sample with double-fractures is established (figure 1) with the parameters as: fracture length 2a = 15 mm, width 2b = 2 mm, inclination angle α = 45°, length of rock bridge L = 10 mm, inclination angle of rock bridge β = 45°. The loading plate rate is controlled by writing FISH commands, with a dynamic loading rate of 3.0×10^3 mm/s.

Table 1. Mesoscopic parameters in the Linearpbond model.

Minimum radius of particles (mm)	Particle size ratio	Particle density (kg.m^{-3})	Particle contact modulus (GPa)	Particle stiffness ratio	Particle friction coefficient	Parallel bond modulus (GPa)	Parallel bond stiffness ratio	Normal bond strength (MPa)	Tangential bond strength (MPa)
0.15	1.72	3169	30	1.5	0.5	45	1.5	80±30	80±30

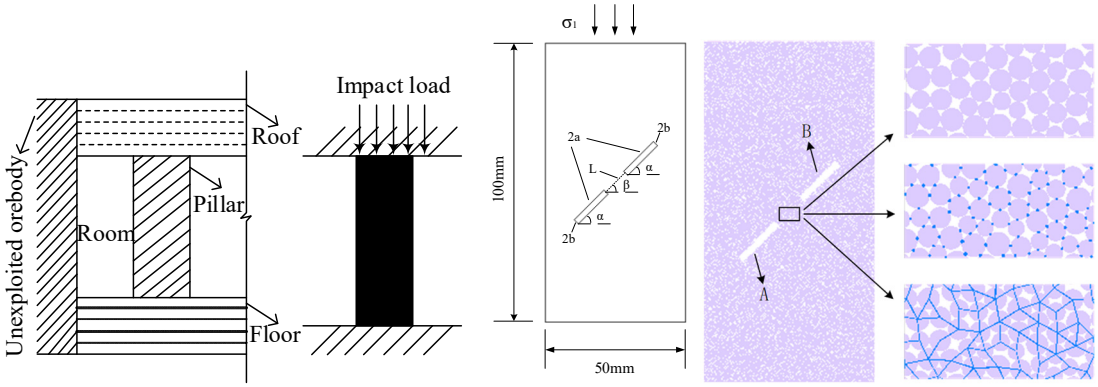

(a) Geomechanical model of rock pillar[1]. (b) Sample plane. (c) Numerical model. (d) Contact mode.

Figure 1. Schematic diagram of the numerical model.

2.2 The experiment schemes for numerical simulation

For the rock sample with double-fractures (figure 1), the fracture at lower end is fracture A, and the fracture at upper end is fracture B. The parameters of fracture A remain constant, and effect of the length of fracture B on failure characteristics of rock sample is explored. The specific schemes are shown in table 2.

Table 2. Simulation schemes and parameters.

Scheme number	Fracture angle α (°)	Fracture length 2a (mm)	Fracture width 2b (mm)	Rock bridge length L (mm)	Rock bridge dip β (°)
I	45	5	2	10	45
II	45	10	2	10	45
III	45	15	2	10	45
IV	45	20	2	10	45
V	45	25	2	10	45

3. Damage and failure characteristics of rock with double-fractures

Figure 2 shows the damage and failure of rock under fracture B with different lengths. The wing crack is marked as a-type, the tip secondary quasi coplanar crack is marked as b-type, and the inclined secondary non-coplanar crack is marked as c-type. From figure 2, the damage characteristics of the rock sample are as follows:

(1) Fracture B, 2a = 5, 10, 15 mm. Fracture A and B begin to be overlapped with b-type, and the a-type crack are brought together to form a crack extended zone extending to both ends of the rock sample. The a-type and c-type cracks mainly occur on the lower left side of fracture A, and b-type cracks mainly occur on the top right side of fracture B.

(2) Fracture B, 2a = 20, 25 mm. After the rock bridge is connected, only the upwardly extending crack extended zone appeared. The a, b and c-type cracks mainly occur on the upper right end of the fracture B, and the a, b-type cracks are mainly occur on the lower left end of the fracture A.

It is observed from figure 3 and figure 5 that the longer the fracture B, the smaller the peak strength is. It is easy for rock sample with long fractures to be reached peak strength under impact load q. Since the speed of microcracks generation is greatly accelerated after peak strength, its stability is not as good as rock sample with short fractures. Therefore, the rock sample with long fractures is more prone to be instability and failure, and its bearing capacity is also relatively low. As shown in figure 4, the comparison of required time for stress reaching the peak strength is as: scheme V < scheme IV < scheme III < scheme II < scheme I, which also shows that the rock sample with short fractures has higher bearing capacity.

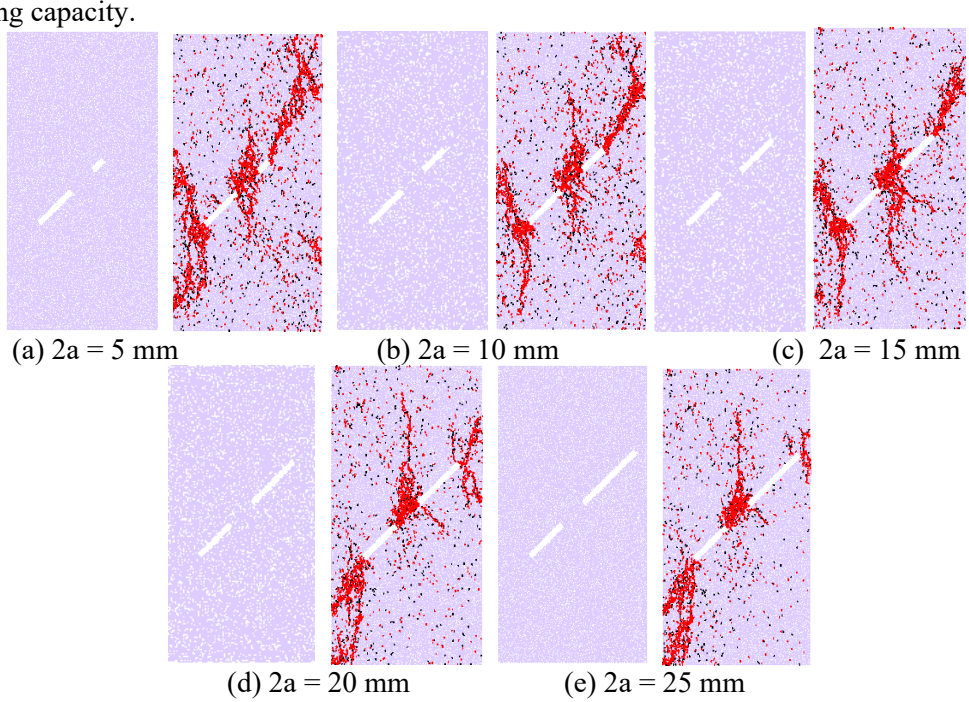

(a) 2a = 5 mm (b) 2a = 10 mm (c) 2a = 15 mm

(d) 2a = 20 mm (e) 2a = 25 mm

Figure 2. Damage and failure of rock sample.

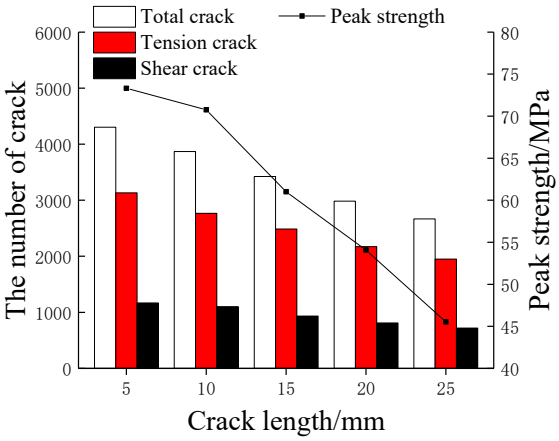

Figure 3. Peak strength and crack statistics for fracture B with different lengths.

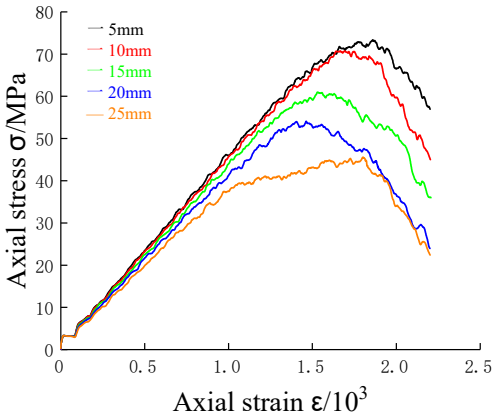

Figure 4. Comparison of stress - strain curves.

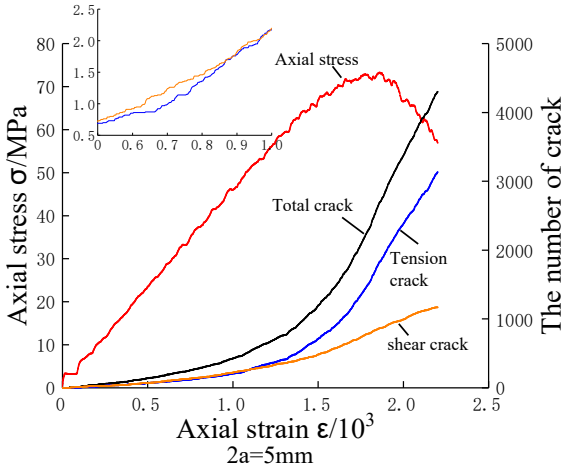

(a)

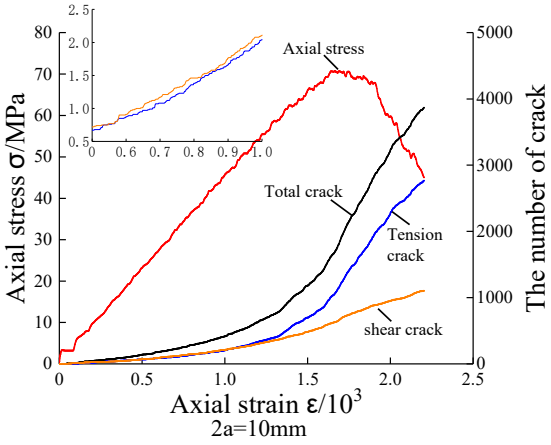

(b)

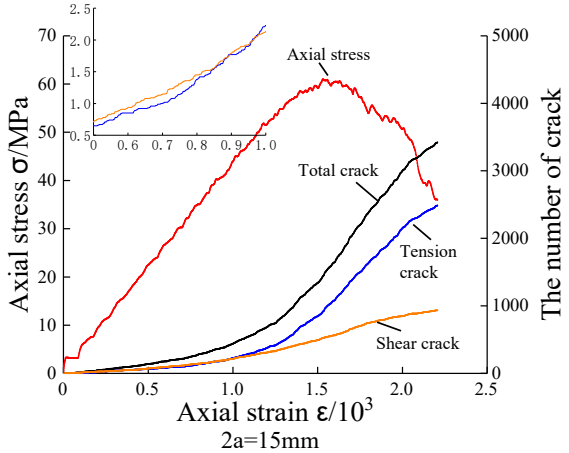

(c)

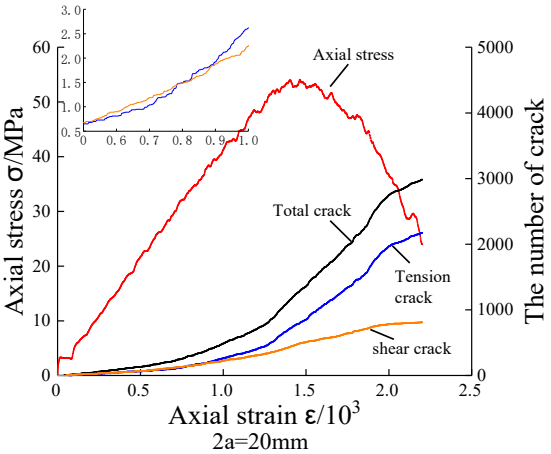

(d)

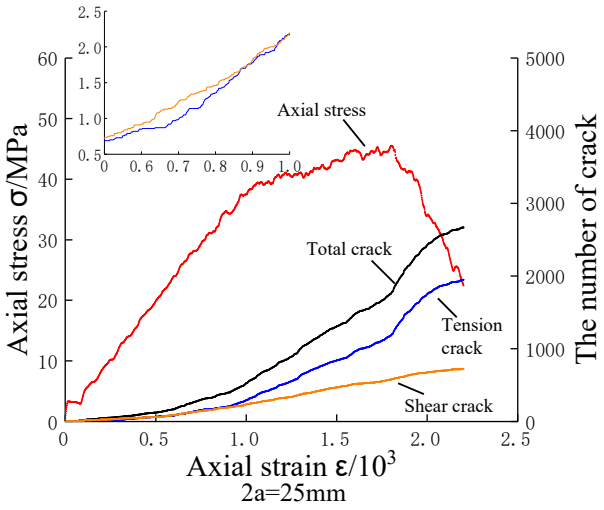

(e)

Figure 5. Variations of stress, crack and strain for different lengths of fracture B.

4. Damage of rock sample and energy evolution

From the point of view of fracture and damage mechanics, due to the complexity of rock, different fracture combinations are helpful to discover the damage mechanism of rock with single crack or multiple cracks, and to understand transfixion way between cracks. Based on fracture mechanism of particle bonding in PFC, the ratio of number of fractured bonds (C_d) to number of total bonds (C) between the particles is defined as the mesoscopic damage variable (D):

$$D = \frac{C_d}{C} \tag{1}$$

where D is the mesoscopic damage variable, C is the number of total bonds, and C_d is the number of fractured bonds.

Energy can be tracked in PFC. The recorded energy include boundary energy (Eboundary), strain energy of parallel bond (Epbstrain), particle sliding energy (Eslip) and particle strain energy (Estrain). Additionally, elastic strain energy (W_e) is defined as:

$$W_e = W_{pb} + W_s \tag{2}$$

where W_e is the elastic strain energy, W_{pb} is the strain energy of parallel bond, and W_s is the particle strain energy.

Table 3 shows the damage and energy statistics for fracture B with different lengths.

Table 3. Damage and energy statistics of rock sample for fracture B with different lengths.

Length 2a (mm)	Number of bonds C	Number of broken bonds C_d	Number of micro-cracks	Total energy (N.m)	W_e at the peak (N.m)	D (10^2)
5	57685	2405	4301	771.21	293.48	4.17
10	57559	2168	3872	710.02	264.14	3.77
15	57417	1891	3422	606.32	204.74	3.29
20	57281	1728	2985	499.65	169.32	3.02
25	57147	1423	2668	451.12	130.60	2.49

It can be seen from table 3 that the number of microcracks is positively correlated with the mesoscopic damage variable D, and the elastic strain energy accumulated at peak is negatively

correlated with the length of fracture B. Figure 7 shows that as the length of rock crack increases, D and peak strength of rock sample decrease. The number of microcracks on rock sample with long fractures post peat is also greatly accelerated.

When the rock fracture is long, a small impact load (q) can make stress reach to the peak strength, causing instability of rock sample. The rock sample with small-size fractures has better stability and stronger bearing capacity, because more energy will be absorbed when it reaches the peak strength.

Beyond the peak strength, W_e is converted to Eslip, and Eslip will drive the relative sliding of internal structures in rock sample, causing fractured bonds and more microcracks. The more the number of fractures, the larger the mesoscopic damage variable D is. The larger the W_e, the more Eslip is converted, and the more the number of microcracks drived, which can explain why the number of microcracks of the damaged rock sample with small-size fractures is greater.

W_e was converted to Eslip after the peak strength, which is the internal cause for the acceleration of the number of post-peak cracks. When the value of Eslip is large enough, a part of the energy is used to drive the rock sample to produce microcracks, and another part makes the rock sample unstable.

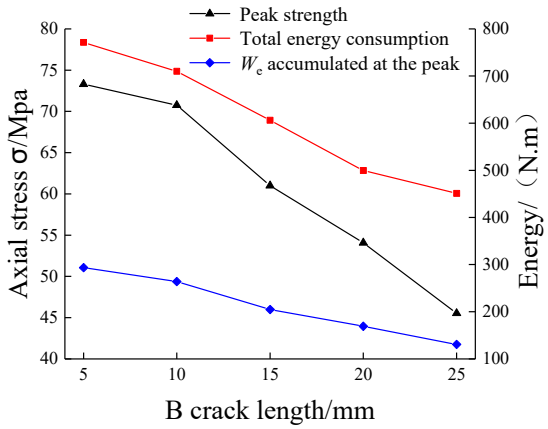

Figure 6. Changes in stress, energy and strain under fracture B with different lengths.

5. Conclusions

(1) The damage and failure of rock with double-fractures under uniaxial dynamic compression is mainly caused by tensile cracks. The peak strength is positively correlated with the number of total cracks on the damaged rock sample. The bearing capacity of the rock sample with short fractures is higher than that with long fractures.

(2) The mesoscopic damage variable (D) was defined. The number of microcracks is positively correlated with the mesoscopic damage variable, while the elastic strain energy (W_e) accumulated at peak and the peak strength are all negatively correlated with the length of fracture B.

(3) The internal cause for the accelerated increase of the number of microcracks post peak was revealed. Because W_e is converted to Eslip after peak, and Eslip drives relative sliding of internal structures in the rock sample, which leads to fractured bonds and more microcracks.

Acknowledgments

This work was supported by the Natural Science Foundation of China (No. 51504091) and the Natural Science Foundation of Hunan Province, China (No. 2018JJ3166). The authors also gratefully acknowledge the helpful comments and suggestions of the reviewers, which have improved the document.

References

[1] Li, X.B., Li, D.Y., Guo, L. (2007) Study on mechanical response of highly-stressed pillars in deep mining under dynamic disturbance. Chinese Journal of Rock Mechanics and Engineering, 26(5): 922-928.

[2] Wang, R.K., Mei, F.D. (2016) Study on mechanical response of highly-stressed pillars under dynamic disturbance. Chinese Journal of Underground Space and Engineering, 12(02): 349-355.
[3] Li, L.Y., Xu, F.G., Gao, F., et al. (2005) Fracture mechanics analysis of rock bridge failure mechanism. Chinese Journal of Rock Mechanics and Engineering, 24(23): 4328-4334.
[4] Pu, C.Z., Cao, P., Yi, Y.L. (2012) Fracture for rock-like materials with two transfixion fissures under uniaxial compression. Journal of Central South University, 43(7): 2708-2716.
[5] Pu, C.Z., Cao, P., Zhao, Y.L. (2010) Numerical analysis and strength experiment of rock-like materials with multi-fissures under uniaxial compression. Rock and soil mechanics, 31(11): 3661-3666.
[6] Deng, Q.H., Hu, S.X., Xue, Y.Q., et al. (2017) Particle flow simulation of uniaxial compression failure of prefabricated cracked rock. Water Resources and Power, (11): 95-98.
[7] Chen, X.Y. (2015) Effect of single closed central fissure on failure characteristics of cracked rock under uniaxial compression. Journal of Yangtze River Scientific Research Institute, 32(9): 104-110.
[8] Tian, W.L., Yang, S.Q., Huang, Y.H. (2017) PFC2D simulation on crack evolution behavior of brittle sandstone containing two coplanar fissures under different confining pressures. Journal of Mining and Safety Engineering, 34(6): 1207-1215.
[9] Li, F., Li, X.F. (2013) Micro-numerical simulation on mechanism of fracture coalescence between two pre-existing flaws arranged in echelon. Journal of Shenzhen University (Science & Engineering), 30(2): 190-194.
[10] Cao, R.H., Cao, P., Lin, H., et al. (2017) Failure characteristics of intermittent fissures under a compressive-shear test: experimental and numerical analyses. Theoretical & Applied Fracture Mechanics, 96: 740-757.